

# Interband tunneling in nanowires with diamond cubic or zincblende crystalline structure based on atomistic modeling

Pino D'Amico\*, Paolo Marconcini, Gianluca Fiori, Giuseppe Iannaccone  
*Dipartimento di Ingegneria dell'Informazione: Elettronica, Informatica,  
Telecomunicazioni, Università di Pisa, Via Caruso 16, I-56100 Pisa, Italy*

We present an investigation of band-to-band tunneling in nanowires with a diamond cubic or zincblende crystalline structure, as a function of cross section and longitudinal electric field. Results are obtained from quantum transport simulations based on non-equilibrium Green's functions with a tight-binding atomistic Hamiltonian. Interband tunneling is extremely sensitive to the longitudinal electric field, to the nanowire cross section, through the gap, and to the material. We have derived an approximate analytical expression for the transmission probability based on WKB theory and on a proper choice of the effective interband tunneling mass, which shows good agreement with results from atomistic quantum simulation.

Conventional field-effect transistors (FETs) are based on the modulation of thermionic injection of charge carriers from the source by tuning the potential barrier between channel and source via the voltage applied on the gate electrode. A crucial parameter in FETs is the sub-threshold swing  $S$  - defined as the gate voltage variation required for a tenfold increase of the drain current. In the ideal case of perfect electrostatic control, when the potential in the channel exactly follows the gate voltage,  $S$  is limited by the tail of the Maxwell-Boltzmann distribution to  $k_B T \ln 10$ , where  $k_B$  is Boltzmann's constant and  $T$  is the temperature.

At room temperature, the intrinsic limitation on  $S$  is therefore  $S \geq 60$  mV/decade, which represents a real threat to continuous integration of semiconductor technology, due to conflicting constraints. Indeed, supply voltage ( $V_{DD}$ ) reduction must accompany device size scaling to keep power consumption per unit area ( $\propto V_{DD}^2$ ) under control, and digital logic still requires the ratio of the current of the device in the on state to be at least  $10^4$  larger than than in the off state, effectively requiring the threshold voltage  $V_{th} \geq 4S$ .

A promising option to reformulate this trade-off is to use a device based on a modified operating principle such as the tunnel FET (TFET) [1]. In a TFET the gate voltage allows to modulate the band-to-band tunneling (BTBT) current between source and channel, by modulating the width of the energy window in which tunneling can take place. In this way, both ends of the allowed energy window for transport are defined by conduction and valence band edges, and the previously discussed limitation on  $S$  is therefore removed, allowing further reduction of  $V_{DD}$ . Several experimental and theoretical works have been dedicated to explore various options for tunnel FETs. [2–6]

Two aspects are important for good performance of TFETs. On the one hand, currents in the on state must

be large for obtaining small delay times, shifting one's preference to lower gap semiconductors, when BTBT can be large. On the other hand, electrostatic control of the potential in the channel via the gate voltage must be ideal, not to unduly lose the advantage on  $S$ , as can be obtained in ultra-thin-body or gate-all-around devices.

In this letter, we investigate the dependence of band-to-band tunneling on nanowire diameter, material, and longitudinal electric field in the interband tunneling barrier, in order to understand their role in determining the achievable BTBT current, to allow comparison of different material systems and channel geometry, and to provide reliable quantities for use in device models at a higher level of abstraction.

We perform atomistic simulations based on a  $sp^3d^5s^*$  Hamiltonian for diamond cubic or zincblende crystals. In particular, we focus on germanium and indium arsenide - which are interesting candidates for TFETs for their relatively small gap as bulk materials - and on silicon, as a reference material for maximum ease of integration with CMOS technology. Nanowire transport is computed in the framework of non-equilibrium Green's functions (NEGFs). Finally, we propose a simple analytical expression derived from the Wentzel-Kramers-Brillouin (WKB) approximation with an ad-hoc tunneling effective mass, that is able to quantitatively reproduce results from atomistic quantum transport simulations and can be used for device modeling at a higher level of abstraction.

In Fig. 1(a) we show an example of a transversal cross section of a zincblende nanowire with the axis oriented in the [001] direction. We use a tight-binding Hamiltonian with a  $sp^3d^5s^*$  first-nearest neighbour representation, where 10 atomic orbitals are considered (spin orbit coupling is neglected). This representation is among the most accurate descriptions available and it is the most used for refined numerical calculations [7–9]. It also gives quantitative agreement with experimental results [10].

We have developed a tool to handle generic Hamiltonians with an arbitrary number of atomic orbitals. In order to speed-up the calculation of the transmission probabilities, we have optimized the tool exploiting the four-

---

\*Present address: S3 CNR-NANO, Via Campi 213/A, I-41125 Modena, Italy email:pino.damico@nano.cnr.it

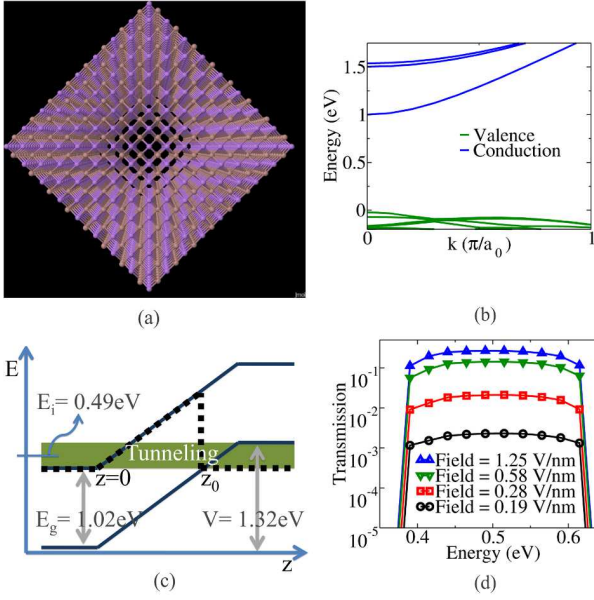


Figure 1: Example of the investigated structures and its main properties: InAs squared nanowire with diameter of 3.4 nm: (a) lattice structure of the (001) plane transversal to the tunneling direction of the wire; (b) band structure of the nanowire; (c) band edge profile considered for the calculation of the tunneling coefficient; the tunneling energy window is highlighted; (d) transmission coefficient in the tunneling window as a function of energy for different values of the longitudinal electric field.

atomic-layer periodicity of zincblende materials in the [001] direction.

The computation of transmission is based on the use of non-equilibrium Green's functions, using a recently developed closed-form method for the calculation of the lead self-energies.[12] Due to the complexity of the investigated structures, a closed-form self-energy scheme was required to reduce the computing time with respect to iterative procedures. In particular, the adopted procedure has been demonstrated to be ten times faster than the Sancho-Rubio iterative method. [13]

The transmission probability is obtained with the well known formula

$$T = Tr[\mathbf{G}^r \cdot \mathbf{\Gamma}_L \cdot \mathbf{G}^a \cdot \mathbf{\Gamma}_R], \quad (1)$$

where  $\mathbf{G}^{r,a}$  are the retarded and advanced Green's function matrices and  $\mathbf{\Gamma}_{L,R}$  represent the tunneling-rate matrices for the left and right lead, respectively. A detailed description of the NEGF transport theory can be found in the literature.[14]

To investigate the possible use of nanowires with zincblende crystalline structure as channels for tunnel FETs we have computed the transmission coefficient due to band-to-band tunneling. We first compute the dispersion relations of the nanowire under investigation as shown in Fig. 1(b), in order to extract the energy gap. Then, we apply a linear potential as shown in

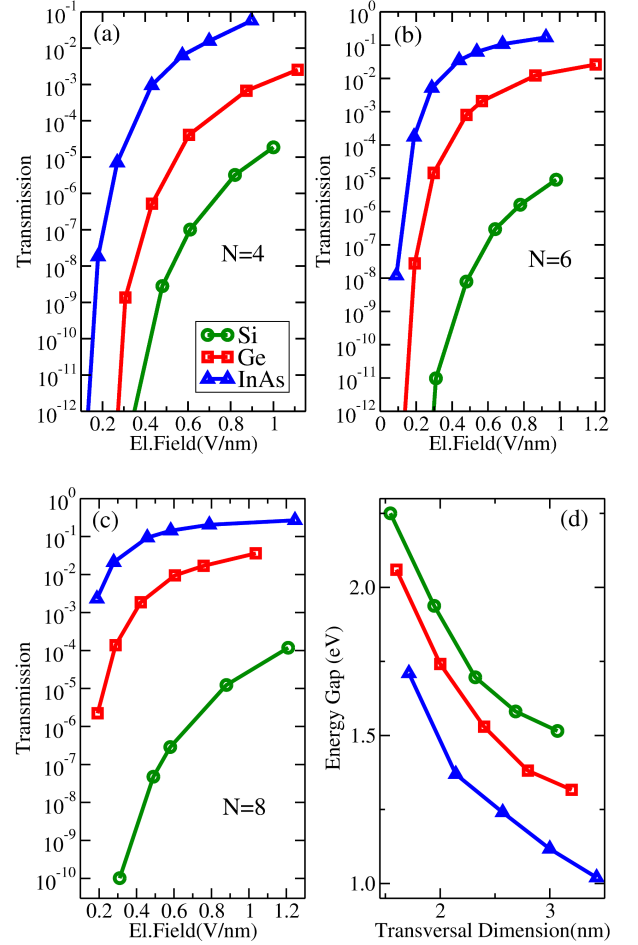


Figure 2: The plateau of transmission probability as a function of the longitudinal electric field is shown for nanowires along the [001] direction, with square cross section of side  $l = a_0 \frac{\sqrt{2}}{2} N$  with  $N = 4$  (a),  $N = 6$  (b),  $N = 8$  (c), where  $a_0$  is the lattice constant ( $a_0 = 5.43, 5.65, 6.05 \text{ \AA}$ ) for Si, Ge, and InAs, respectively). In every plot the transmission coefficient is shown for three different materials: Si, Ge and InAs. (d) dependence of the energy gap on  $l$ , for the different materials, extracted from the dispersion relation.

Fig. 1(c) with an end-to-end potential drop larger than  $E_g$  in order to open an inter-band tunneling window of 0.3 eV. This ensures limited mismatch and a transmission probability almost independent of energy, as shown in Fig. 1(d), where transmission probability exhibits a plateau in the interband tunneling energy window. In the following analysis, we use the value of the transmission coefficient in such plateau as a metrics for comparing interband tunneling among different materials and as a function of the applied longitudinal field.

Nanowire tunnel FETs pose different tradeoffs: a smaller nanowire cross section implies a better electrostatic control, and therefore a better subthreshold behavior. On the other hand, it also implies a larger gap, and therefore a smaller tunneling current in the on state. To

explore this tradeoff from a quantitative point of view for different materials, we consider nanowires in which propagation occurs along the [001] direction, and the lateral surfaces are on {110} planes, as shown in Fig. 1(a).

The side of the square cross section  $l$  is determined by an integer parameter  $N$  according to the formula  $l = a_0 \frac{\sqrt{2}}{2} N$  where  $a_0$  is the lattice constant for the material under investigation ( $a_0 = 5.43, 5.65, 6.05 \text{ \AA}$ ) for Si, Ge and InAs, respectively). In Fig. 2 we show results for  $N = 4, 6, 8$ , corresponding to a side  $l$  between roughly 1.5 nm and 3 nm depending on the material. As can be seen in Fig. 2(d), with increasing cross section area the gap rapidly decreases, causing a very steep increase of the tunneling probability. In addition, as can be seen from Figs. 2(a)-(c) the transmission coefficient increases by several orders of magnitude for an increase of the longitudinal electric field of just one order of magnitude. In the case of InAs, in particular, for the nanowire with  $l \approx 3$  nm, the transmission probability can be very high, opening the possibility for very large ON currents.

As we pointed out before, full band calculations, as the ones presented here, are computationally very demanding for diamond cubic and zinblende nanowires. It is therefore interesting to verify whether simplified expressions are reliable in predicting the behavior of the tunneling coefficient. In Fig. 3 a comparison between the transmission probability plateau obtained from the atomistic NEGF calculation and the WKB results is shown. The WKB transmission coefficient is obtained with the formula

$$T_{\text{WKB}} = \exp \left[ -2 \int_0^{z_0} \sqrt{\frac{2m}{\hbar^2} Fz} dz \right], \quad (2)$$

where  $F$  is the longitudinal electric field and  $m = m_0 \cdot m_*$  is the effective mass in the interband tunneling barrier plotted in Fig. 3(d) ( $m_0$  is the electron mass at rest). The potential profile is linear with the slope given by the applied electric field, as shown in Fig. 1(c). The integration region is determined by  $z_0 = E_g/F$ . After few manipulations the formula (2) can be approximated as follows:

$$T_{\text{WKB}} = \exp \left[ -\frac{20}{3} m_*^{\frac{1}{2}} \frac{E_g^{\frac{3}{2}}}{F} \right], \quad (3)$$

where  $E_g$  is expressed in eV and  $F$  in V/nm. With (3) we fit the numerical results for InAs and Ge, choosing the effective masses in two different ways: for InAs, which exhibits two clear well-separated conduction and valence bands, the effective mass is simply obtained from the second derivative of the first conduction band profile. For Ge the effective mass is just a fitting parameter, because multiple quasi-degenerate conduction and valence bands are present. The values of the masses are shown in Fig. 3(d). For Si, in order to reproduce the atomistic NEGF results for the tunneling probability, we have modified the functional dependence of the WKB transmission

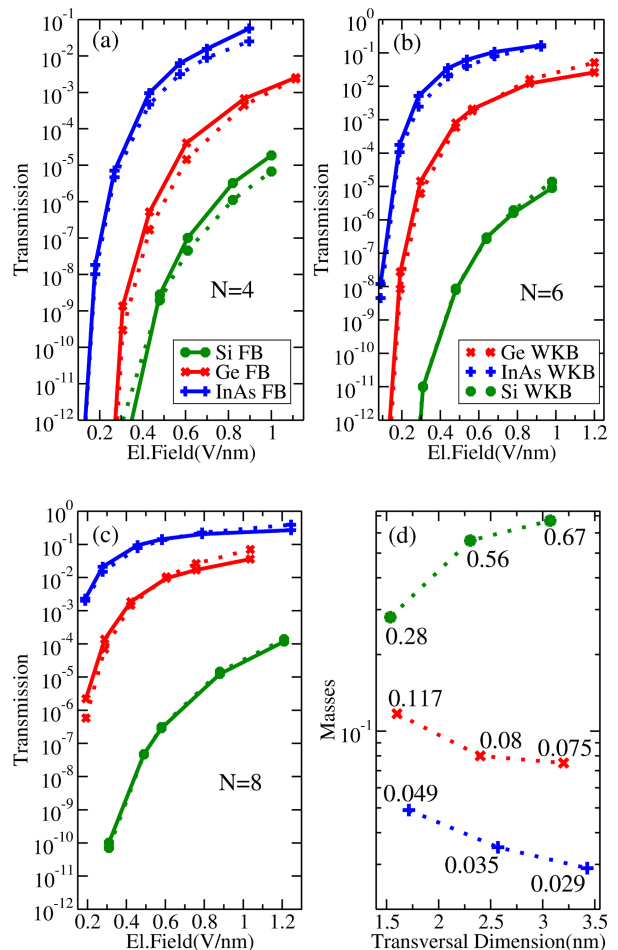


Figure 3: Comparison between the transmission probability plateau obtained from the atomistic NEGF calculation (solid lines) and the WKB results (dotted lines). Nanowires with three different cross section sides  $l$  are considered:  $l = a_0 \frac{\sqrt{2}}{2} N$  with  $N = 4$  (a),  $N = 6$  (b),  $N = 8$  (c). The values of effective masses used for the WKB approximation are shown in (d); they have been extracted from the energy-band profile of the corresponding atomistic calculation for InAs and as a fitting parameter for Ge and Si.

probability on the electric field using the formula

$$T_{\text{WKB}}^{\text{Si}} = \exp \left[ -\frac{20}{3} m_*^{\frac{1}{2}} \frac{E_g^{\frac{3}{2}}}{F^{0.71}} \right]. \quad (4)$$

We have then used the effective mass as a fitting parameter (values shown in Fig. 3(d)). As can be seen, the simplified formulas of Eqs. (3,4) reproduce quite accurately full-band calculations for InAs, Ge and Si respectively. A more complex implementation of the WKB approximation could in principle be used to obtain better accuracy [15], but our results show that the simplest version can still provide a very good quantitative agreement. Therefore, first-principle numerically accurate calculations can be reproduced by simple analytical

formulas, with effective masses extracted from the band profile of the atomistic structure or from fitting procedures. This makes self-consistent calculations of currents a much less demanding computational task compared to full-band NEGF calculations.

We have investigated diamond cubic or zincblende nanowires for different materials and for different cross sections up to a side of 3.4 nm using atomistic Hamiltonians based on  $sp^3d^5s^*$  tight-binding representation.

The extreme sensitivity of the tunneling probability to the electric field and to the cross section side provides a hint of the sensitivity of the tunnel FET ON current to the variability of the nanowire cross section and to the presence of random charged defects in the nanowire region where interband tunneling takes place. We have shown that tunneling probabilities between 0.01 and 0.1 -

suitable for achieving reasonable ON currents in TFETs - can be obtained with longitudinal electric field close to 1 V/nm (still smaller than the dielectric breakdown field) in InAs for  $l > 1.5$  nm and for Ge for  $l > 3$  nm. We have also shown that full-band calculations are quantitatively reproduced by simple formulas derived from the WKB approximation, considering an ad hoc interband tunneling mass.

Finally, the presented results - obtained with rigorous quantum transport simulations based on an atomistic tight binding Hamiltonian - can be used as input for semiclassical modeling of electron devices, where interband tunneling has to be represented with a synthetic scattering rate.

Support from the EC through the FP7 STEEPER Project (contract n. 257267) is gratefully acknowledged.

- 
- [1] W. Hansch, C. Fink, J. Schulze, and I. Eisele, *Thin Solid Films* **369**, 387 (2000).
  - [2] T. Nirschl, P.-F. Wang, C. Weber, J. Sedlmeir, R. Heinrich, R. Kakoschke, K. Schröder, J. Holz, C. Pacha, T. Schulz, M. Ostermayr, A. Olbrich, G. Georgakos, E. Ruderer, W. Hansch, and D. Schmitt-Landsiedel, *Electron Device Meeting, IEDM Technical Digest. IEEE International*, pag. 195 (2004).
  - [3] K. K. Bhuiwarka, J. Schulze, and I. Eisele, *IEEE Trans. Electron Devices* **52**, 909 (2005).
  - [4] W. Y. Choi, B.-G. Park, J. D. Lee, and T.-J. K. Liu, *IEEE EDL* **28**, 743 (2007).
  - [5] K. Boucart, and A. M. Ionescu, *IEEE Trans. Electron Devices* **54**, 1725 (2007).
  - [6] G. Fiori, and G. Iannaccone, *IEEE Electron Devices Lett.* **30**, 1096 (2009).
  - [7] J. C. Slater and G. F Koster, *Phys. Rev.* **94**, 1498 (1954).
  - [8] T. B. Boykin, G. Klimeck, R. C. Bowen, and F. Oyafuso, *Phys. Rev. B* **66**, 125207 (2002).
  - [9] T. B. Boykin, G. Klimeck, and F. Oyafuso, *Phys. Rev. B* **69**, 115201 (2004).
  - [10] K. Ganapathi, Y. Yoon, and S. Salahuddin, *Appl. Phys. Lett.* **97**, 033504 (2010).
  - [11] M. Luisier, A. Schenck, W. Fichtner, and G. Klimeck, *Phys. Rev. B* **74**, 205323 (2006).
  - [12] M. Wimmer, <http://epub.uni-regensburg.de/12142/>, PhD Thesis (2009).
  - [13] M. P. Lopez Sancho, J. M. Lopez Sancho, and J. Rubio, *J. Phys. F* **15**, 851 (1985).
  - [14] D. A. Ryndyk, R. Gutiérrez, B. Song, and G. Cuniberti, *Springer Series in Chemical Physics*, **93**, 213 (2009).
  - [15] M. Luisier and G. Klimeck, *J. Appl. Phys.* **107**, 084507 (2010).